Int. j. adv. multidisc. res. stud. 2026; 6(6):232-239

Received: 14-09-2026
Accepted: 24-10-2026

International Journal of Advanced Multidisciplinary Research and Studies

ISSN: 2583-049X

Analysis of the Effect of Belimbing Wuluh Leaf Extract (Averrhoa Bilimbi L.) as a Green Inhibitor on Corrosion Rate and Validation of Optimized Operating Conditions in a Circulating Cooling Water System

[1] Al Swendo Musbar, [2] Eko Ariyanto, [3] Elfidiah

[1, 2, 3] Department of Chemical Engineering, Faculty of Engineering, Universitas Muhammadiyah Palembang, Jl. Jend. Ahmad Yani 13 Ulu, Palembang, 30263, Indonesia

DOI: https://doi.org/10.62225/2583049X.2026.6.6.7124

Corresponding Author: **Al Swendo Musbar**

Abstract

Corrosion and fouling in circulating cooling water systems can reduce equipment performance. This study evaluates star fruit (Averrhoa bilimbi L.) leaf extract as a green corrosion inhibitor using the weight loss method and optimizes operating conditions through Response Surface Methodology (RSM) based on Central Composite Design (CCD). Inhibitor concentrations of 0, 6, 8, 10, 12, and 14 g/L were evaluated at temperatures of 25–55°C and stirring speeds of 100–400 rpm. Surfaces were characterized using Fourier Transform Infrared Spectroscopy (FTIR), Scanning Electron Microscopy (SEM), and Energy-Dispersive X-ray (EDX) analysis. The tannin content of the extract was 0.0223% (w/w). Increasing inhibitor concentration reduced the corrosion rate, with 14 g/L achieving 1.697 mpy and 71% inhibition efficiency. The observed corrosion rates ranged from 1.9319 to 5.7682 mpy. The lowest corrosion rate, 1.9319 mpy, was obtained at 55°C and 200 rpm. FTIR identified O–H, C=O, and C–O functional groups, while SEM–EDX indicated reduced surface deterioration and formation of an organic protective layer. RSM–CCD and ANOVA predicted optimum conditions at 54.53°C and 212.86 rpm, with a predicted corrosion rate of 1.9673 mpy. These findings demonstrate the potential of star fruit leaf extract as an environmentally friendly inhibitor for circulating cooling water systems.

Keywords: Green Inhibitor, Averrhoa Bilimbi, Corrosion Rate, Cooling Water, Weight Loss, Response Surface Methodology, Central Composite Design

1. Introduction

Oleochemical industries require reliable utility systems to maintain stable operating conditions and continuous production. Cooling water systems, particularly indirect cooling water (ICW), are widely used to remove heat from process equipment such as heat exchangers, condensers, and reactors. The effectiveness of these systems is strongly influenced by water quality, heat-transfer conditions, and operating parameters. In industrial cooling systems, inadequate control of water chemistry and operating conditions can promote corrosion, scaling, and fouling, which may reduce heat-transfer efficiency, accelerate material degradation, and increase maintenance requirements (Wang *et al*., 2023; Lu *et al*., 2024; Ye *et al*., 2021) [15, 7, 16].

Corrosion is one of the major degradation mechanisms affecting metallic components in circulating cooling water systems. The corrosion process is influenced by several interacting parameters, including water chemistry, dissolved oxygen, aggressive ions, temperature, pH, and hydrodynamic conditions. In particular, chloride ions and dissolved species can increase the electrochemical activity of metallic surfaces, while temperature and fluid movement influence reaction kinetics and mass transfer at the metal–water interface (Wang *et al*., 2023; Lu *et al*., 2024; Zhang *et al*., 2022) [15, 7, 17]. Consequently, controlling corrosion in circulating cooling water requires not only chemical treatment but also consideration of the operating conditions under which the inhibitor is applied. Corrosion inhibitors are commonly used to reduce the interaction between corrosive media and metallic surfaces. Their effectiveness generally involves adsorption or formation of a protective film that limits anodic and cathodic reactions. Conventional cooling-water treatment commonly relies on synthetic chemical inhibitors; however, concerns regarding environmental impact, chemical consumption, and sustainability have encouraged the development of environmentally benign alternatives. Plant-derived extracts have received considerable attention because they

contain organic compounds with functional groups capable of interacting with metallic surfaces and forming protective adsorption layers (Chaovanalikit & Wrolstad, 2004; Ye *et al*., 2021; Chauhan *et al*., 2022) [2, 16, 3].

Averrhoa bilimbi L., commonly known as star fruit, is one plant that has potential as a green corrosion inhibitor. Its leaves contain secondary metabolites such as flavonoids, tannins, saponins, and other phenolic compounds. These compounds contain functional groups capable of interacting with metal surfaces and potentially contributing to the formation of a protective layer. Previous studies have demonstrated the phytochemical and biological potential of A. bilimbi leaf extracts, indicating that the plant contains compounds that can support its application in environmentally oriented material-protection systems (Hari *et al*., 2020; Safitri & Leliqia, 2021; Sakib *et al*., 2024) [5, 10, 11]. In particular, Bangera *et al*. reported that A. bilimbi leaf extract exhibited corrosion-inhibition potential for mild steel, demonstrating the feasibility of using the plant as a sustainable inhibitor (Bangera *et al*., 2022) [1].

Previous studies have also demonstrated that plant extracts can reduce corrosion rates under different corrosive environments. Zulkaham and Dahlan reported that increasing the concentration and immersion time of guava leaf extract improved corrosion inhibition efficiency for stainless steel (Zulkaham & Dahlan, 2023) [18]. Taqwa *et al*. (2021) [14] demonstrated that papaya leaf extract could improve the corrosion resistance of carbon steel in crude-oil environments under variations in temperature and immersion time (Taqwa *et al*., 2021) [14]. More broadly, studies on plant-based corrosion inhibitors have emphasized the importance of adsorption, surface interaction, and the chemical characteristics of the extract in determining inhibition performance (Chaovanalikit & Wrolstad, 2004; Ye *et al*., 2021; Chauhan *et al*., 2022) [2, 16, 3]. However, many previous investigations have been conducted using synthetic corrosive solutions or laboratory conditions that do not fully represent the complexity of industrial circulating cooling water.

The operating conditions of cooling-water systems introduce an additional challenge because temperature and hydrodynamic conditions can simultaneously influence corrosion kinetics, mass transfer, oxygen transport, and inhibitor adsorption. Increasing fluid movement may enhance the transport of dissolved oxygen and aggressive ions toward the metal surface, whereas temperature affects the kinetics of electrochemical reactions and the stability of protective films (Wang *et al*., 2023; Zhang *et al*., 2022) [15, 17]. Therefore, evaluating inhibitor performance at a single operating condition may not adequately describe its behavior under industrially relevant conditions. A systematic evaluation of temperature and stirring speed is consequently required to identify the operating region that provides the lowest corrosion rate. Although previous studies have investigated plant extracts as green corrosion inhibitors, studies integrating a natural inhibitor with actual circulating cooling water, surface characterization, and statistical optimization of operating conditions remain limited. In particular, the combined relationship between inhibitor concentration, corrosion response, surface morphology, and the interaction of temperature and hydrodynamic conditions requires further investigation. Surface characterization using Fourier Transform Infrared Spectroscopy (FTIR), Scanning Electron Microscopy (SEM), and Energy-Dispersive X-ray Spectroscopy (EDX) can provide complementary evidence regarding functional groups, surface morphology, elemental composition, and the formation of protective deposits (Sapanathan *et al*., 2021; Pratama *et al*., 2023; Fonna *et al*., 2021) [13, 9, 4]. In addition, Response Surface Methodology (RSM) provides a systematic statistical approach for evaluating the individual, quadratic, and interaction effects of process variables and for determining optimum operating conditions (Myers *et al*., 2021; Koohestani *et al*., 2021; Salimi *et al*., 2023) [8, 6, 12].

This study therefore investigates the performance of Averrhoa bilimbi L. leaf extract as a green corrosion inhibitor in a circulating cooling water system. The effect of inhibitor concentration on corrosion rate and inhibition efficiency is evaluated using the weight loss method. The effects of temperature and stirring speed are subsequently investigated to assess the influence of operating conditions on corrosion behavior. FTIR, SEM, and EDX analyses are employed to support the interpretation of the inhibition mechanism and surface changes. Finally, Response Surface Methodology based on Central Composite Design (RSM–CCD) is applied to determine the optimum combination of temperature and stirring speed for minimizing corrosion rate. The study aims to provide an integrated experimental and statistical approach for developing a more environmentally sustainable corrosion-control strategy for industrial circulating cooling water systems.

2. Experimental Section

The materials used in this study consisted of Averrhoa bilimbi L. leaves as the raw material for green corrosion inhibitor preparation, industrial circulating cooling water (Indirect Cooling Water/ICW) as the corrosive medium, utility water, distilled water, ethanol at concentrations of 70% and 96%, and metal specimens used for the corrosion test. The A. bilimbi leaf extract was prepared using 70% ethanol as the extraction solvent, while 96% ethanol was used during specimen preparation and cleaning. The ICW was obtained from the industrial circulating cooling-water system and used as the test medium to represent the actual operating environment. The metal specimens were prepared to evaluate corrosion behavior through the weight-loss method.

The equipment used included a hot plate, rotary evaporator, visible spectrophotometer, analytical balance, blender, oven, measuring cylinders, beakers, volumetric flasks, droppers, funnels, Petri dishes, evaporating dishes, aluminum foil, abrasive paper, filter paper, and tissue. The blender was used to reduce the particle size of the leaf material, while the oven was used for drying. The rotary evaporator was used to concentrate the ethanolic extract after maceration. The analytical balance was used to determine the mass of the leaf material and metal specimens, whereas the visible spectrophotometer was used for spectrophotometric analysis of the tannin content. Glassware and filtration equipment were used during the preparation and treatment of the extract and test solutions, while abrasive paper and ethanol were used to prepare and clean the metal specimens before the corrosion test.

The Averrhoa bilimbi L. leaves were first dried and ground into a fine powder. A total of 1.2 kg of powdered leaves was subjected to maceration using 70% ethanol for three days. The maceration process was continued until the solvent changed in color, indicating the extraction of compounds

from the plant material. The resulting extract solution was filtered using filter paper, and the filtrate was collected and concentrated using a rotary evaporator at 50 °C to remove the ethanol solvent and obtain a concentrated leaf extract. The concentrated extract obtained from 1.2 kg of powdered leaves had a mass of 185.54 g and was subsequently used for phytochemical screening, tannin analysis, and corrosion inhibition testing.

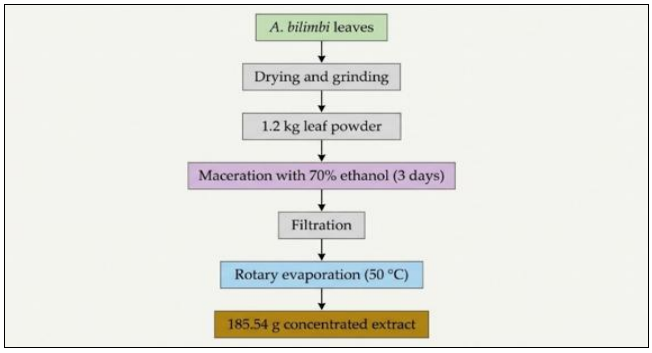


Fig 1: Flow Diagram of A. Bilimbi Leaf Extraction

Phytochemical screening was performed to identify the major secondary metabolites present in the Averrhoa bilimbi L. leaf extract, including flavonoids, saponins, tannins, alkaloids, and triterpenoids. Tannin identification was additionally performed using a ferric chloride ($FeCl_3$) test, in which 1% $FeCl_3$ solution was added to the extract. The formation of a greenish-black precipitate was used as an indication of the presence of tannins. The tannin content was subsequently determined using a Folin–Ciocalteu spectrophotometric method based on the procedure reported by Chaovanalikit and Wrolstad (Chaovanalikit & Wrolstad, 2004) [2]. A tannic acid standard solution was prepared at a series of concentrations, and each standard solution was reacted with Folin–Ciocalteu reagent followed by sodium carbonate solution. After the required incubation period, the absorbance was measured at 765 nm using a visible spectrophotometer. A calibration curve was constructed by plotting absorbance against tannic acid concentration, and the tannin content of the extract was calculated from the resulting regression equation. The calibration curve obtained was $y = 0.00496x + 0.00555$, with $R^2 = 0.9983$, corresponding to a tannin content of 0.0223% (w/w).

The metal specimens were prepared with dimensions of 3 cm × 2 cm × 0.28 cm. Prior to the corrosion test, the specimen surfaces were mechanically polished using 1000-grit abrasive paper to remove surface impurities and obtain a relatively uniform surface condition. The specimens were then cleaned with 96% ethanol, dried, and weighed using an analytical balance to obtain the initial mass. The specimens were immersed in industrial circulating cooling water (ICW) containing Averrhoa bilimbi L. leaf extract at inhibitor concentrations of 0, 6, 8, 10, 12, and 14 g/L. The corrosion tests were conducted at temperatures of 25, 35, 45, and 55 °C and stirring speeds of 100, 200, 300, and 400 rpm for 28 days. After the immersion period, the specimens were removed, cleaned, dried, and weighed again to determine the mass loss. The corrosion rate was subsequently calculated based on the mass loss of the specimens, while the inhibition efficiency was determined by comparing the corrosion rate in the presence of the inhibitor with that of the uninhibited system.

The corrosion rate was determined using the weight-loss method by measuring the difference between the initial and final masses of the metal specimens after the immersion period. The corrosion rate was expressed in mils per year (mpy) and calculated based on the specimen mass loss, exposed surface area, metal density, and immersion time. The inhibition efficiency was calculated from the reduction in corrosion rate obtained in the presence of the Averrhoa bilimbi L. leaf extract compared with the corrosion rate of the uninhibited specimen. The corrosion rate and inhibition efficiency values were used as the response variables for evaluating the effectiveness of the green inhibitor under the tested operating conditions.

The corrosion rate was determined using the weight-loss method by measuring the difference between the initial and final masses of the metal specimens after the 28-day immersion period. The weight loss was calculated using Equation (1):

$$W = W_o - W_f$$

Where (W) is the weight loss of the specimen (g), (Wo) is the initial specimen mass (g), and (Wf) is the final specimen mass (g). The corrosion rate was expressed in mils per year (mpy) and calculated using Equation (2):

$$CR = \frac{365 \times 1.000 \times W}{D \times A \times T \times (2{,}54)^3}$$

Where (CR) is the corrosion rate (mpy), (W) is the weight loss (g), (A) is the exposed surface area of the specimen (cm^2), (D) is the metal density (g/cm^3), and (T) is the immersion time (days). The inhibition efficiency was calculated using Equation (3):

$$IE\ (\%) = \frac{C1 - C2}{C1} \times 100\%$$

Where (CR1) is the corrosion rate of the uninhibited system (mpy) and (CR2) is the corrosion rate in the presence of the inhibitor (mpy). The resulting corrosion rate and inhibition efficiency values were used to evaluate the effectiveness of the Averrhoa bilimbi L. leaf extract as a green corrosion inhibitor.

Response Surface Methodology (RSM) with a Central Composite Design (CCD) was applied to determine the optimum operating conditions for minimizing the corrosion rate. The RSM analysis was performed after selecting the inhibitor concentration of 14 g/L as the optimum concentration based on the weight-loss corrosion test. Two process variables were evaluated, namely temperature and stirring speed, while the corrosion rate was used as the response variable. The temperature was varied from 25 to 55 °C and the stirring speed from 100 to 400 rpm. The CCD consisted of 13 experimental runs, including repeated center-point experiments at 40 °C and 250 rpm, to evaluate the reproducibility of the experimental response. The experimental data were analyzed using analysis of variance (ANOVA), and the mathematical model was used to describe the relationship between temperature and stirring speed and the corrosion rate. The optimum operating conditions were determined by minimizing the predicted corrosion rate within the experimental range.

Table 1: Central Composite Design and Experimental Conditions

Run	Temperature (°C)	Stirring Speed (RPM)	Corrosion Rate (mpy)
1	40	250	2.9461
2	25	100	2.4984
3	40	250	2.9461
4	55	400	3.6612
5	40	100	5.3336
6	25	400	3.6646
7	40	250	2.9461
8	55	250	2.1796
9	25	250	3.0815
10	40	250	2.9461
11	40	250	2.9461
12	40	400	3.3718
13	55	100	2.9112

The corrosion products and specimen surfaces were characterized using Fourier Transform Infrared Spectroscopy (FTIR), Scanning Electron Microscopy (SEM), and Energy Dispersive X-ray Spectroscopy (EDX). FTIR analysis was performed on powdered deposits obtained from the specimen surface after exposure to the circulating cooling water to identify the functional groups associated with the corrosion products and deposited material. The FTIR spectrum was recorded over the wavenumber range of 4000–400 cm^{-1} and expressed in transmittance (%T). SEM analysis was used to examine changes in the surface morphology of the metal specimens before and after exposure to the circulating cooling water. EDX analysis was performed in conjunction with SEM to determine the elemental composition of the specimen surface. The characterization results were used to complement the weight-loss measurements and to provide supporting information on surface morphology, elemental composition, and functional groups associated with the corrosion products.

The experimental data obtained from the RSM–CCD design were statistically analyzed using analysis of variance (ANOVA) at a 95% confidence level, with a significance level of 0.05. A cubic model was selected to describe the relationship between temperature, stirring speed, and corrosion rate because the experimental response showed nonlinear behavior and higher-order interactions between the process variables. The adequacy of the developed model was evaluated based on the coefficient of determination (R^2), adjusted R^2, predicted R^2, analysis of variance, and Adequate Precision. Model terms with a p-value less than 0.05 were considered statistically significant. The optimum operating condition was determined using the desirability function by setting corrosion rate as the response to be minimized. Model validation was performed by comparing the corrosion rate predicted by the RSM model at the optimum condition with the corresponding experimental corrosion rate within the investigated operating range. The agreement between the predicted and experimental responses was evaluated based on the difference between the two values and the percentage deviation.

3. Result and Discussion

3.1 Extraction and Phytochemical Screening of Averrhoa bilimbi L. Leaf Extract

The maceration process using 70% ethanol for three days produced 185.54 g of concentrated Averrhoa bilimbi L. leaf extract from 1,200 g of dried leaf powder, corresponding to an extraction yield of 15.46%. The extract was dark brown to black in appearance. The relatively high extraction yield indicates that the ethanol maceration process was effective in extracting soluble compounds from the leaf material. Phytochemical screening showed the presence of several secondary metabolites, including saponins, alkaloids, flavonoids, tannins, and triterpenoids. The presence of tannins was confirmed by the formation of a dark green to black coloration after the addition of 1% $FeCl_3$. These secondary metabolites, particularly compounds containing heteroatom-bearing functional groups, may contribute to the adsorption of inhibitor molecules onto the metal surface and consequently influence the corrosion inhibition process (Quraishi *et al*., 2022).

Table 2: Phytochemical Screening Results of Averrhoa bilimbi L. Leaf Extract

Sample Name	Sample Condition	Parameter		Result	Analysis Technique
Averrhoa bilimbi L. Leaf	Extract	Saponin		+++++	A foam layer with a height of 1 cm was formed
		Alkaloid	Dragendoff	+++++	A brick-red solution was formed
			Mayer	+	A light-brown precipitate was formed
			Wagner	+++++	A brown-colored solution was formed
		Flavonoid		+++++	A yellowish solution was formed
		Tanin	Fecl3 1%	+++++	A green to dark-green solution was formed
		Triterpenoid		+++	A yellow solution was formed

3.2 Tannin Content Analysis

The tannin content of the Averrhoa bilimbi L. leaf extract was determined using the Folin–Ciocalteu spectrophotometric method. The analysis was performed using a calibration curve obtained from the standard solution, with absorbance measured at a wavelength of 765 nm. The resulting calibration curve was expressed by the regression equation (y = 0.00496x + 0.00555), with a coefficient of determination (R2) of 0.9983, indicating a strong linear relationship between the standard concentration and absorbance. Based on the calibration equation, the tannin content in the Averrhoa bilimbi L. leaf extract was determined to be 0.0223% (w/w). The presence of tannins is relevant to the corrosion inhibition performance of the extract because tannin molecules contain oxygen-bearing functional groups that can interact with the metal surface and contribute to the formation of a protective layer.

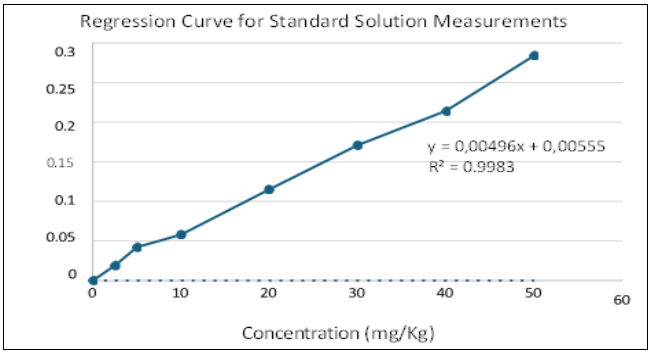


Fig 2: Calibration curve for tannin content determination of Averrhoa bilimbi L. leaf extract

3.3 Effect of Inhibitor Concentration on Corrosion Rate

The effect of Averrhoa bilimbi L. leaf extract concentration on the corrosion rate was evaluated using the weight-loss method. As shown in Fig 3, the corrosion rate decreased progressively with increasing inhibitor concentration. In the

absence of inhibitor (0 g/L), the corrosion rate was 5.904 mpy. Increasing the inhibitor concentration to 6, 8, 10, and 12 g/L reduced the corrosion rate to 3.770, 3.0189, 1.978, and 1.974 mpy, respectively. The lowest corrosion rate was obtained at 14 g/L, with a value of 1.697 mpy and an inhibition efficiency of 71%. The relationship between inhibitor concentration and corrosion rate was represented by the linear regression equation ($y = -0.3151x + 5.6831$), with ($R^2 = 0.956$), indicating a strong inverse relationship between inhibitor concentration and corrosion rate. The decrease in corrosion rate can be attributed to the increasing availability of active compounds in the leaf extract, which can adsorb onto the metal surface and form a protective film that limits the interaction between the metal and corrosive species (Quraishi *et al*., 2022).

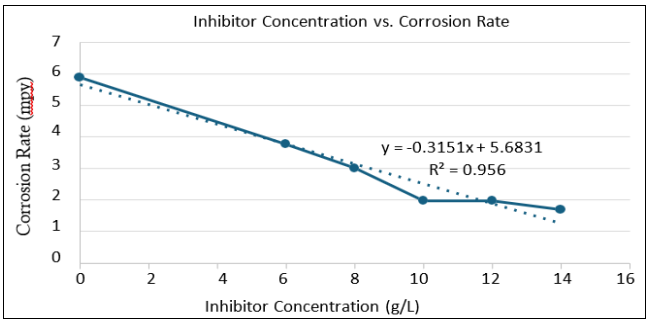


Fig 3: Effect of Averrhoa bilimbi L. leaf extract concentration on corrosion rate

3.4 Effect of Temperature and Stirring Speed on Corrosion Rate

The effects of temperature and stirring speed on the corrosion rate were evaluated at the optimum inhibitor concentration of 14 g/L over a 28-day immersion period. The corrosion rate varied with the combination of temperature and stirring speed, indicating that the two operating variables jointly influenced the corrosion response. The highest corrosion rate was 5.7682 mpy at 35 °C and 100 rpm, whereas the lowest value was 1.9319 mpy at 55 °C and 200 rpm. At 200 rpm, the corrosion rate decreased consistently with increasing temperature, from 3.1166 mpy at 25 °C to 2.9681 mpy at 35 °C, 2.6943 mpy at 45 °C, and 1.9319 mpy at 55 °C. In contrast, the other stirring speeds showed more fluctuating responses. This behavior indicates that the effect of temperature on corrosion rate depended on the stirring condition, suggesting an interaction between temperature and hydrodynamic conditions in the corrosion system.

Table 3: Corrosion Rate at Different Temperatures and Stirring Speeds

Temperature (°C)	100 rpm	200 rpm	300 rpm	400 rpm
25	2.4984	3.1166	3.0464	3.6646
35	5.7682	2.9681	2.9050	3.6024
45	4.8991	2.6943	3.2172	3.1413
55	2.9112	1.9319	2.4272	3.6612

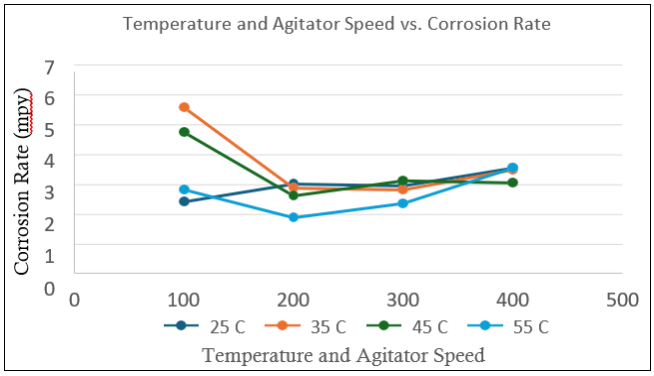


Fig 4: Effect of Temperature and Stirring Speed on Corrosion Rate

3.5 Surface Characterization by SEM and EDX

Surface characterization was performed using Scanning Electron Microscopy (SEM) and Energy Dispersive X-ray Spectroscopy (EDX) to evaluate morphological changes and elemental composition of the metal specimens after exposure to circulating cooling water. SEM observations showed that the initial specimen had a relatively compact surface with longitudinal grooves and a rough texture, whereas the specimen after corrosion exposure exhibited a rougher, granular, heterogeneous, and agglomerated morphology. These changes indicate the accumulation of corrosion products and deposits on the metal surface during exposure to the circulating cooling water. EDX analysis of the corroded specimen showed that the surface was dominated by carbon (42.95 mass%), iron (36.42 mass%), and oxygen (14.62 mass%), with smaller amounts of phosphorus, zinc, calcium, copper, aluminum, chlorine, silicon, manganese, and nickel. The presence of Fe and O indicates the contribution of iron-based corrosion products, while the multielement composition reflects the complex nature of deposits formed during exposure to the circulating cooling water (Fonna *et al*., 2021) [4].

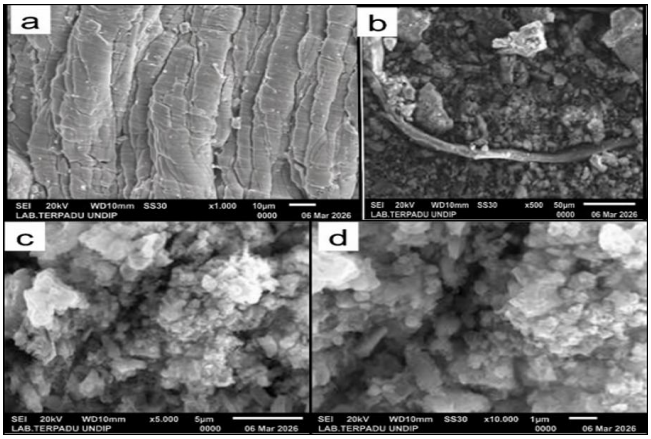


Fig 5: SEM images of the metal specimen: (a) initial condition before corrosion testing; (b) condition after corrosion exposure at ±500× magnification; (c) condition after corrosion exposure at ±5,000× magnification; and (d) condition after corrosion exposure at ±10,000× magnification

Table 4: Elemental Composition of the Metal Specimen after Corrosion Exposure

Element	Mass (%)
C	42.95
O	14.62
Al	0.30
Si	0.16
P	2.18
Cl	0.17
Ca	0.79
Mn	0.15
Fe	36.42
Ni	0.14
Cu	0.79
Zn	1.34
Total	**100.00**

3.6 FTIR Analysis of Corrosion Products

FTIR analysis was conducted to identify the functional groups present in the corrosion deposits collected from the metal specimen after exposure to circulating cooling water. The spectrum was recorded over the wavenumber range of 4000–400 cm^{-1} and showed ten main absorption bands at 3748.40, 3320.95, 1625.13, 1455.72, 1359.36, 1314.78, 1018.30, 817.67, 700.99, and 480.99 cm^{-1}. The prominent bands at 3320.95, 1625.13, and 1018.30 cm^{-1} were associated with O–H, C=C/C=O, and C–O functional groups, respectively. The broad absorption in the lower-wavenumber region, particularly around 480.99 cm^{-1}, may be associated with metal–oxygen vibrations, including a possible Fe–O contribution. The FTIR results therefore indicate the presence of both oxygen-containing organic groups and inorganic components in the corrosion deposit. However, FTIR alone cannot specifically identify the iron oxide phases formed, and further phase characterization such as XRD or Raman spectroscopy would be required for definitive identification (Hari *et al*. 2020) [5].

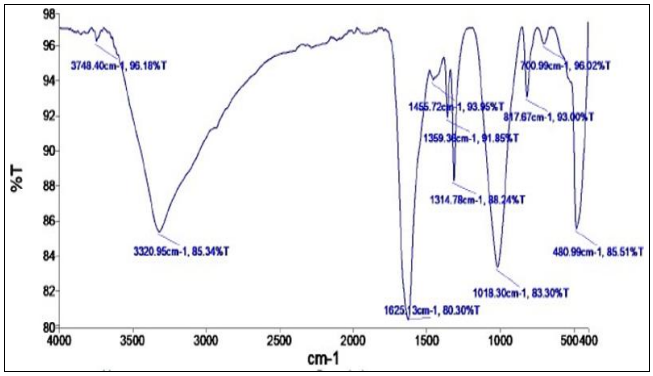


Fig 6: FTIR spectrum of the corrosion deposit showing the main absorption bands at 3320.95 cm^{-1} (O–H), 1625.13 cm^{-1} (C=C/C=O), and 1018.30 cm^{-1} (C–O)

3.7 RSM–CCD Modeling and ANOVA

Response Surface Methodology (RSM) based on Central Composite Design (CCD) was used to evaluate the effects of temperature and stirring speed on the corrosion rate at an inhibitor concentration of 14 g/L [20]. A cubic model was selected to describe the nonlinear relationship between the process variables and the corrosion response. The analysis of variance (ANOVA) showed that the developed model was statistically significant, with an F-value of 9.19 and a p-value of 0.0133, indicating significance at the 95% confidence level. Among the model terms, stirring speed (B), the quadratic terms of temperature (A^2) and stirring speed (B^2), and the interaction term A^2B were statistically significant, with p-values of 0.0072, 0.0124, 0.0034, and 0.0031, respectively. In contrast, the linear temperature term (A) and the linear interaction term (AB) were not statistically significant at $p < 0.05$. The model produced an (R^2) of 0.9279 and an adjusted (R^2) of 0.8269, indicating that the model explained 92.79% of the variation in the experimental corrosion-rate response. The Adequate Precision value of 12.6869, which exceeded the recommended value of 4, indicated an adequate signal-to-noise ratio within the design space. However, the predicted (R^2) value of −7.3821 indicates limited predictive capability when assessed using the predicted (R^2) criterion; therefore, the model performance should be interpreted primarily based on its fit to the experimental data and its subsequent validation at the optimum condition.

Table 5: Analysis of Variance (ANOVA) for the Cubic Model of Corrosion Rate

Source	Sum of Squares	df	Mean Square	F-value	p-value
Model	6.46	7	0.9227	9.19	0.0133
A – Temperature	0.4067	1	0.4067	4.05	0.1003
B – Stirring speed	1.92	1	1.92	19.16	0.0072
AB	0.0433	1	0.0433	0.4312	0.5404
A^2	1.46	1	1.46	14.55	0.0124
B^2	2.73	1	2.73	27.21	0.0034
A^2B	2.84	1	2.84	28.30	0.0031
AB^2	0.4082	1	0.4082	4.06	0.0999
Residual	0.5022	5	0.1004	–	–
Lack of Fit	0.5022	1	0.5022	–	–
Pure Error	0.0000	4	0.0000	–	–
Cor Total	6.96	12	–	–	–

3.8 Optimization and Experimental Validation

Optimization was performed using the desirability function by setting the corrosion rate as the response to be minimized. The optimum operating condition was obtained at a temperature of 54.53 °C and a stirring speed of 212.86 rpm, with a predicted minimum corrosion rate of 1.9673 mpy and a desirability value of 1.000. The optimum condition was located within the experimental design space and represents the combination of process variables predicted to provide the minimum corrosion rate. The predicted response was subsequently compared with the best experimental result, which was a corrosion rate of 1.9319 mpy obtained at 55 °C and 200 rpm. The difference between the predicted and experimental values was 0.0354 mpy, corresponding to a deviation of approximately 1.83% relative to the experimental value. The relatively small difference indicates that the RSM optimization result was close to the experimentally observed optimum and adequately represented the corrosion response within the investigated operating range.

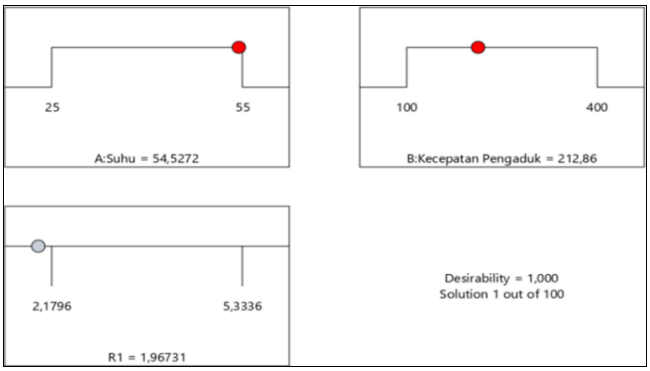


Fig 7: Desirability function for optimization of temperature and stirring speed to minimize corrosion rate

The comparison between the RSM-predicted and experimentally obtained corrosion rates is presented in Table 6.

Table 6: Comparison of RSM-Predicted and Experimental Corrosion Rates

Condition	Temperature	Condition	Temperature
RSM optimum	54.53	212.86	1.9673
Best experimental condition	55.00	200	1.9319
Difference	–	–	0.0354
Deviation	–	–	1.83%

4. Conclusion

4.1 Conclusion

The Averrhoa bilimbi L. leaf extract demonstrated potential as a green corrosion inhibitor for circulating cooling water. Phytochemical screening confirmed the presence of saponins, alkaloids, flavonoids, tannins, and triterpenoids, while the tannin content was determined to be 0.0223% (w/w). Increasing the inhibitor concentration generally reduced the corrosion rate, with the lowest corrosion rate of 1.697 mpy and an inhibition efficiency of 71% obtained at an inhibitor concentration of 14 g/L. At this concentration, variations in temperature and stirring speed produced corrosion rates ranging from 1.9319 to 5.7682 mpy.

RSM–CCD optimization predicted an optimum operating condition at 54.53 °C and 212.86 rpm, with a predicted corrosion rate of 1.9673 mpy and a desirability value of 1.000. The predicted optimum was compared with the best experimental condition tested in this study, namely 55 °C and 200 rpm, which produced an experimental corrosion rate of 1.9319 mpy. The difference between the predicted and experimental corrosion rates was 0.0354 mpy, corresponding to a deviation of approximately 1.83% relative to the experimental value. Although the experimental condition was not identical to the numerical RSM optimum, the small deviation indicates that the RSM prediction was consistent with the experimental response within the investigated operating range. SEM–EDX and FTIR characterization further supported the formation of corrosion products and the presence of oxygen-containing functional groups on the exposed surface.

4.2 Suggestion

Further research is recommended to investigate the long-term stability and performance of Averrhoa bilimbi L. leaf extract under actual circulating cooling water operating conditions. Future studies may also evaluate the effects of water-quality parameters, such as pH, conductivity, hardness, and dissolved ions, on inhibitor performance. Additional surface and electrochemical characterization is recommended to further clarify the corrosion inhibition mechanism and the interaction between inhibitor compounds and the metal surface.

5. References

1. Bangera KV, *et al*. Averrhoa bilimbi Leaf Extract as a Potent and Sustainable Inhibitor for Mild Steel in 1 M HCl Medium: Experimental and DFT Enumeration. Chemistry Africa. 2022; 5(2):341-358. Doi: https://doi.org/10.1007/s42250-022-00313-8
2. Chaovanalikit A, Wrolstad RE. Total anthocyanins and total phenolics of fresh and processed cherries and their antioxidant properties. Journal of Food Science. 2004; 69(1):FCT67-FCT72. Doi: https://doi.org/10.1111/j.1365-2621.2004.tb17858.x
3. Chauhan DS, Quraishi MA, Sorour S. Experimental and theoretical approaches for corrosion inhibition studies. Surfaces and Interfaces. 2022; 28:101665. Doi: https://doi.org/10.1016/j.surfin.2021.101665
4. Fonna S, *et al*. Investigation of corrosion products formed on surface of carbon steel in cooling water system. Heliyon. 2021; 7:e06608. Doi: https://doi.org/10.1016/j.heliyon.2021.e06608
5. Hari A, *et al*. A comparative FTIR spectroscopic assessment of leaf extract in Averrhoa bilimbi and Averrhoa carambola. Life Sciences International Research Journal. 2020; 7(1):61-69.
6. Koohestani S, *et al*. Central composite design optimization of acid red 18 dye adsorption. Sustainability. 2021; 13(5):2515. Doi: https://doi.org/10.3390/su13052515
7. Lu S, *et al*. Electrochemical effects on carbon steel in circulating cooling water systems: Scaling, corrosion and chemicals synergies. Journal of Water Process Engineering. 2024; 63:105337. Doi: https://doi.org/10.1016/j.jwpe.2024.105337
8. Myers RH, Montgomery DC, Anderson-Cook CM. Response surface methodology: Process and product optimization using designed experiments (5th ed.). Wiley, 2021. Doi: https://doi.org/10.1002/9781118916018
9. Pratama R, *et al*. Biofilm formation and organic deposits in palm oil cooling systems: A SEM-EDX analysis. Journal of Oleochemical Engineering. 2023; 15(2):45-60.
10. Safitri R, Leliqia NPE. Review of phytochemical properties of Averrhoa bilimbi leaves and fruit. Journal of Pharmaceutical Science and Application. 2021; 3(1):32-39. Doi: https://doi.org/10.24843/JPSA.2021.v03.i01.p04
11. Sakib MN, *et al*. Isolation and characterization of secondary metabolites from Averrhoa bilimbi. Bangladesh Journal of Botany. 2024; 53(1):115-122. Doi: https://doi.org/10.3329/bjb.v53i1.72254
12. Salimi S, *et al*. Application of RSM for corrosion prediction and optimization. Materials Today Communications. 2023; 35:105624.
13. Sapanathan T, *et al*. Surface morphology and microstructural evolution of Fe-based alloy during mechanical preparation and SEM characterization. Materials Today: Proceedings. 2021; 46:1882-1887. Doi: https://doi.org/10.1016/j.matpr.2020.09.596

14. Taqwa FM, Irwan I, Pardi P. Penggunaan ekstrak daun pepaya sebagai inhibitor korosi pada baja. Jurnal Teknologi. 2021; 21(1):6-11. Doi: https://doi.org/10.30811/teknologi.v21i1.2193
15. Wang Y, *et al*. Effect of temperature and flow velocity on corrosion behavior of carbon steel in cooling water systems. Corrosion Science. 2023; 216:111089.
16. Ye X, *et al*. Flow accelerated corrosion behavior of carbon steel in cooling water environment. Engineering Failure Analysis. 2021; 120:105084. Doi: https://doi.org/10.1016/j.engfailanal.2020.105084
17. Zhang Y, Gao X, Zhou Y. Effect of hydrodynamic conditions on corrosion behavior of carbon steel in aqueous environments. Corrosion Science. 2022; 198:110123.
18. Zulkaham NA, Dahlan D. Ekstrak daun jambu bol (Syzygium malaccense) sebagai inhibitor korosi pada kawat ortodontik. Jurnal Fisika Unand. 2023; 12(2):323-328. Doi: https://doi.org/10.25077/jfu.12.2.322-327.2023